

Crystallization Behavior of Mixtures of Fatty Acid Ethyl Esters with Ethyl Stearate

L. Boros,[†] M. L. S. Batista,[‡] Raquel V. Vaz,[‡] B. R. Figueiredo,[‡] V. F. S. Fernandes,[‡] M. C. Costa,^{†,§}
M. A. Krahenbuhl,[†] A. J. A. Meirelles,[§] and J. A. P. Coutinho^{*,‡}

[†]LPT, Department of Chemical Processes (DPQ), School of Chemical Engineering (FEQ), University of Campinas (UNICAMP), P.O. Box: 6066, 13083-970, Campinas, São Paulo, Brazil, [‡]CICECO, Departamento de Química da Universidade de Aveiro, 3810-193 Aveiro, Portugal, and [§]EXTRA, Department of Food Engineering (DEA), School of Food Engineering (FEA), University of Campinas (UNICAMP), P.O. Box 6121, 13083-862, Campinas, São Paulo, Brazil

Received April 24, 2009. Revised Manuscript Received July 2, 2009

In spite of their interest to understand the low-temperature behavior of biodiesel, data on the crystallization behavior of fatty acid esters mixtures are scarce. To overcome this limitation, the melting points of seven binary mixtures of saturated and unsaturated fatty acid ethyl esters with ethyl stearate were measured by differential scanning calorimetry (DSC) and are here reported. The Predictive UNIQUAC model, developed for the prediction of cloud points of diesels and previously applied to fatty acid methyl esters, is shown to produce an excellent prediction of the experimental data measured in this work. It is shown that, alternatively, a simple ideal solution is able to describe the melting points with identical accuracy to the Predictive UNIQUAC model and may prove to be able to describe cloud points of real biodiesel.

Introduction

Although most of the energy consumed nowadays still has a fossil origin, the world is quickly recognizing that these energy sources are limited and are associated with environmental hazards resulting from carbon dioxide, sulfur compounds, and NO_x emissions. The impact of these emissions is socially manifest in human health problems, greenhouse effect, and climatic changes. Moreover, fossil fuels often also equate with political instability, and the interest in a reduction of the energetic dependence goes hand-in-hand with the environmental concerns in the quest for alternative and more sustainable energy sources. One of the possibilities to reduce the consumption of fossil fuels is their replacement by biofuels from renewable resources such as bioethanol or biodiesel, among others.

Biodiesel is currently being produced essentially by the transesterification of vegetable oils and fats.¹ It consists in a number of alkali-catalyzed reactions, where the triglycerides are converted into fatty acid esters by reaction with an alcohol (methanol/ethanol), producing glycerol as a secondary product.

The biodiesel properties are dependent on the raw materials used on its synthesis. This biofuel is much less complex than conventional diesels, consisting on a blend of liquid, nontoxic, biodegradable, water immiscible fatty acid esters. Their cold flow performance depends both on the oil and the alcohol used in the transesterification. Biodiesel from cheap vegetable oils, such as palm oil, with large concentration of saturated fatty acid esters, although less vulnerable to oxidation and displaying better lubricating and combustion properties, has a worst behavior at low temperatures, because of its tendency to crystallize.²

In spite of its ecological appeal, with favorable impact on emissions and the energetic independence of the countries,

most biodiesel production is based on the methanolic route that relies on a nonrenewable resource such as methanol. As biofuel, a biodiesel based on fatty acid ethyl esters has the advantage of being entirely based on renewable raw materials, and moreover it displays a higher specific energy, higher cetane index, better lubricity, and enhanced cold flow behavior because of the lower melting points of ethyl esters.^{3,4}

There are several specifications that stipulate the limit values for the low-temperature properties of biodiesel, such as the cloud point, CP (EN 23015, ASTM D-2500); the pour point, PP (ASTM D-97, ASTM D-5949); the cold filter plugging point, CFPP (EN 116, IP-309, ASTM D-6371); and the low temperature filterability test, LTFT (ASTM D-4539).⁵

The CP is the temperature at which a hazy appearance develops on a fuel upon cooling due to the crystallization of the heavier fatty acid esters. With further temperature decrease the crystal particles grow and agglomerate, reducing the capacity of the liquid to flow through porous media, plugging the fuel filters, and eventually gel the fluid, preventing the flow altogether. A biodiesel has, in general, higher CPs than a conventional diesel resulting from the presence of saturated esters on its composition, thus a biodiesel produced from oils or fats with considerable amounts of saturated triglycerides will display high CPs. The presence of solid crystals in the biodiesel affects its viscosity, volatility, flowability, and filterability.

The standards for the CP recommend its measurement in cooling runs, but the measurement of a solid–liquid transition is prone to subcooling. In particular, our experience shows that unlike what was observed with paraffins, the subcooling of mixtures of fatty acid esters are usually of 5–10 K. To avoid

*To whom correspondence should be addressed. E-mail: jcoutinho@ua.pt.

(1) Hanna, M. A.; Ma, F. *Biores. Tech.* **1999**, *70*, 1–15.

(2) Dunn, R. O.; Bagby, M. O. *J. Am. Oil Chem. Soc.* **1995**, *72*, 895.

(3) Lopes, J. C. A.; Boros, L.; Krahenbuhl, M. A.; Meirelles, A. J. A.; Daridon, J. L.; Pauly, J.; Marrucho, I. M.; Coutinho, J. A. P. *Energy Fuels* **2008**, *22*, 747–752.

(4) Foglia, T. A.; Nelson, L. A.; Dunn, R. O.; Marmer, W. N. *J. Am. Oil Chem. Soc.* **1997**, *74*, 951–955.

(5) *Annual Book of ASTM Standards*, Vol. 05.01, 1999.

the subcooling, the measurement of the melting point of crystals present in a solution is preferable, being more accurate and reproducible.⁶ For this reason in this work the measurement of the melting points instead of crystallization temperatures of the mixture was adopted, and we will be referring to the experimental data as melting/cloud points.

Although the cloud point receives less attention than other low-temperature specifications from biodiesel producers, this is the most relevant property of a biodiesel to characterize its low-temperature behavior. The CP is an equilibrium property that can be measured with great accuracy, and it has been shown that for biodiesel both CFPP and LTFT are linear functions of the CP.² Moreover, being an equilibrium property it is possible to develop a thermodynamic model to predict its value from the knowledge of the fluid composition that is routinely obtained by gas chromatography analysis. A thermodynamic model to predict cloud points of biodiesel, and from these the PP, CFPP, and LTFT, would be a very valuable tool for the production planning and formulation of oil blends in biodiesel production. In a previous work³ the Predictive UNIQUAC model was evaluated for the prediction of cloud points of fatty acid methyl esters mixtures and biodiesel. This model will be here applied to the experimental data measured along with a simple approach based on the assumption of pure solid phase and ideal liquid mixture.

Unlike for conventional fuels, for which the complexity of their composition precludes that a simple mixture is studied as representative of these fluids behavior, a B100 biodiesel is a simple fluid that in the limit may have no more than 2 or 3 major different esters and, even in more complex situations such as biodiesel produced from blends of oils, no more than 10 different esters are present in the mixture. The binaries here presented are thus representative of B100 biodiesel, and the results can be safely extrapolated to real biodiesel.

In this work we report experimental data for the melting/cloud points of seven binary mixtures of fatty acid ethyl esters with ethyl stearate. Information concerning the importance of the heavy saturated fatty acid esters on the melting/cloud points of the mixtures are discussed. Two approaches to the prediction of the experimental data are tested with success as shown below.

Experimental Section

Standards used for calibration of the DSC were indium (99.99%), certified by TA Instruments; and cyclohexane (min 99.9%) and naphthalene (min 99%), both from Merck. The high purity fatty acid esters (min 99%), obtained from Nu Check, were used with no further purification. The mixtures were prepared by weight on an analytical balance with a precision of ± 0.2 mg, and the weighted quantities of the components, placed in a glass tube, were heated under stirring in a nitrogen atmosphere to a temperature 10 K above the higher melting point of the pure components.

Thermograms for these mixtures were obtained using a MDSC 2920, TA Instruments calorimeter. The calorimeter was equipped with a refrigerated cooling system, allowing for the operation between 203 and 600 K. Samples (2–5 mg) of each mixture were weighed in a microanalytical balance (Perkin-Elmer AD6) with an accuracy of $\pm 0.2 \cdot 10^{-5}$ mg and sealed in aluminum pans. To erase previous thermal histories, each sample was heated to 15 K above the highest melting temperature of the pure components and kept at this temperature for 20 min. The samples were then

cooled to 25 K below the melting point of the components at a cooling rate of 1 K min⁻¹ and equilibrated at that temperature for 30 min. After this pretreatment, the thermogram of each sample was collected in a heating run, at a heating rate of 1 K min⁻¹.

The accuracy of the experimental melting points of the mixtures was evaluated on the basis of repeated runs performed for the calibration substances and some mixtures. Calibrations of the calorimeter with standards were performed in quintuplicate, with absolute average deviations (AADs) lower than of 0.1 K for all of the standards. On the basis of these experimental runs, the reproducibility of the data was estimated to be no higher than 0.2 K, the uncertainty of the DSC measurements are larger than this value.⁷

Modeling

The description of the crystallization/melting behavior of fatty acid ethyl esters is described here using an approach previously proposed by us for alkane mixtures^{8–22} and also applied to fatty acids and fatty acids methyl esters with success.^{3,23}

The solid–liquid equilibrium is established by the equality of fugacities of each component in the liquid and solid phase

$$f_i^L(T, P, x_i^L) = f_i^S(T, P, x_i^S) \quad (1)$$

The liquid phase fugacity can be obtained from

$$f_i^L(T, P, x_i^L) = P x_i^L \phi_i^L \quad (2)$$

where the fugacity coefficient ϕ_i^L is calculated using the Soave–Redlich–Kwong equation of state (EoS),²⁴ with the LCVM mixing rules.^{25,26} The volumetric properties calculated by the cubic EoS are corrected using the volume translation proposed by Peneloux et al.²⁷

(7) Costa, M. C.; Rolemberg, M. P.; Boros, L. A. D.; Krahenbuhl, M. A.; Oliveira, M. G.; Meirelles, Antonio. J. A. *J. Chem. Eng. Data* **2007**, *52*, 30–36.

(8) Pauly, J.; Daridon, J. L.; Coutinho, J. A. P.; Dirand, M. *Fuel* **2005**, *84*, 453–459.

(9) Sansot, J. M.; Pauly, J.; Daridon, J. L.; Coutinho, J. A. P. *AIChE J.* **2005**, *51*, 2089–2097.

(10) Coutinho, J. A. P.; Gonçalves, C.; Marrucho, I. M.; Pauly, J.; Daridon, J. L. *Fluid Phase Equilib.* **2005**, *233*, 29–34.

(11) Coutinho, J. A. P.; Mirante, F.; Pauly, J. *Fluid Phase Equilib.* **2006**, *247*, 8–17.

(12) Coutinho, J. A. P.; Dauphin, C.; Daridon, J. L. *Fuel* **2000**, *79*, 607–616.

(13) Coutinho, J. A. P. *Energy Fuels* **2000**, *14*, 625–631.

(14) Coutinho, J. A. P.; Daridon, J. L. *Energy Fuels* **2001**, *15*, 1454–1460.

(15) Daridon, J. L.; Pauly, J.; Coutinho, J. A. P.; Montel, F. *Energy Fuels* **2001**, *15*, 730–735.

(16) Pauly, J.; Daridon, J. L.; Coutinho, J. A. P. *Fluid Phase Equilib.* **2001**, *187*, 71–82.

(17) Mirante, F. I. C.; Coutinho, J. A. P. *Fluid Phase Equilib.* **2001**, *180*, 247–255.

(18) Queimada, A. J. N.; Dauphin, C.; Marrucho, I. M.; Coutinho, J. A. P. *Thermochim. Acta* **2001**, *372*, 93–101.

(19) Coutinho, J. A. P.; Mirante, F.; Ribeiro, J. C.; Sansot, J. M.; Daridon, J. L. *Fuel* **2002**, *81*, 963–967.

(20) Pauly, J.; Daridon, J. L.; Sansot, J. M.; Coutinho, J. A. P. *Fuel* **2003**, *82*, 595–601.

(21) Pauly, J.; Daridon, J. L.; Coutinho, J. A. P. *Fluid Phase Equilib.* **2001**, *224*, 237–244.

(22) Coutinho, J. A. P.; Edmonds, B.; Morwood, T.; Szczepanski, B.; Zhang, X. *Energy Fuels* **2006**, *20*, 1081–1088.

(23) Costa, M. C.; Krahenbuhl, M. A.; Meirelles, A. J. A.; Daridon, J. L.; Pauly, J.; Coutinho, J. A. P. *Fluid Phase Equilib.* **2007**, *253*, 118–123.

(24) Soave, G. *Chem. Eng. Sci.* **1972**, *27*, 1197.

(25) Boukouvalas, C.; Spiliotis, N.; Coutsikos, P.; Tzouvaras, N.; Tassios, D. *Fluid Phase Equilib.* **1994**, *92*, 75–106.

(26) Boukouvalas, C. J.; Magoulas, K. G.; Stamataki, S. K.; Tassios, D. P. *Ind. Eng. Chem. Res.* **1997**, *36*, 5454–5460.

(27) Peneloux, A.; Rauzy, E.; Freze, R. *Fluid Phase Equilib.* **1982**, *8*, 7–23.

(6) Bhat, N. V.; Mehrotra, A. K. *Ind. Eng. Chem. Res.* **2004**, *3451–3461*.

Table 1. Thermophysical Properties Used for the Ethyl Esters Studied on This Work

fatty ester	M_w	r	q	T_c/K	P_c/bar	ω	$\Delta_{\text{vap}}H/\text{kJ mol}^{-1}$	$\Delta_{\text{fus}}H/\text{kJ mol}^{-1}$	T_{fus}/K	
ethyl caprilate	C10:0	172	7.525	6.356	656.39	21.60	0.628	58.0	22.40	229.17
ethyl caprate	C12:0	200	8.8738	7.436	690.21	18.46	0.709	67.8	30.23	254.10
ethyl laurate	C14:0	228	10.2226	8.516	719.13	15.97	0.787	77.6	38.07	272.31
ethyl myristate	C16:0	256	11.5714	9.596	744.27	14.02	0.862	87.4	45.91	286.98
ethyl palmitate	C18:0	284	12.9202	10.676	766.41	12.43	0.935	97.2	53.75	297.92
ethyl stearate	C20:0	312	14.269	11.756	786.12	11.12	1.005	107.0	61.60	307.63
ethyl oleate	C20:1	310	14.0369	11.543	771.07	11.12	1.013	107.3	25.39	252.99
ethyl linoleate	C20:2	308	13.8048	11.33	785.89	11.57	1.008	108.9	24.39	220.68

The solid-phase fugacity at a pressure P is obtained from

$$\ln f_i^S(P) = \ln f_i^S(P_0) + \frac{1}{RT} \int_{P_0}^P \bar{v}_i^S dP \quad (3)$$

where the fugacity of the component i in the solid phase at reference pressure P_0 , here taken as the atmospheric pressure, is calculated from its fugacity in the subcooled liquid state at the same temperature T

$$f_i^S(P_0) = x_i^S \gamma_i^S(P_0) f_i^{0,L}(P_0) \exp \left[-\frac{\Delta_{\text{fus}}H_i}{RT} \left(1 - \frac{T}{T_{\text{fus},i}} \right) \right] \quad (4)$$

where γ_i^S represents the activity coefficient of the compound i in the solid phase; and $T_{\text{fus},i}$ and $\Delta_{\text{fus}}H_i$ are, respectively, the fusion temperature and enthalpy of fusion of the pure compound i at the reference pressure. Because the systems studied in this work were measured at atmospheric pressure, the Poynting correction term in eq 3 can be neglected and eq 3 can be written as

$$f_i^S(P) = f_i^S(P_0) = x_i^S \gamma_i^S(P_0) f_i^{0,L}(P_0) \exp \left[-\frac{\Delta_{\text{fus}}H_i}{RT} \left(1 - \frac{T}{T_{\text{fus},i}} \right) \right] \quad (5)$$

The activity coefficients γ_i^S of the solid phase were described by means of the new predictive UNIQUAC model recently proposed.^{11,12} The predictive UNIQUAC model can be written as

$$\frac{g^E}{RT} = \sum_{i=1}^n x_i \ln \left(\frac{\Phi_i}{x_i} \right) + \frac{Z}{2} \sum_{i=1}^n q_i x_i \ln \left(\frac{\theta_i}{\Phi_i} \right) - \sum_{i=1}^n x_i q_i \ln \left[\sum_{j=1}^n \theta_j \exp \left(-\frac{\lambda_{ij} - \lambda_{ii}}{q_i RT} \right) \right] \quad (6)$$

with

$$\theta_i = \frac{x_i q_i}{\sum_j x_j q_j} \quad \text{and} \quad \Phi_i = \frac{x_i r_i}{\sum_j x_j r_j} \quad (7)$$

The predictive local composition concept^{28–32} allows for the estimation of the interaction energies, λ_{ij} , used by this model without fitting to experimental data. The pair interaction energies between two identical molecules are estimated from the enthalpy of sublimation of crystal of the pure component

$$\lambda_{ii} = -\frac{2}{Z} (\Delta_{\text{sub}}H_i - RT) \quad (8)$$

where $Z = 10$ is the coordination number. The enthalpies of sublimation, $\Delta_{\text{sub}}H = \Delta_{\text{vap}}H + \Delta_{\text{fus}}H$ are calculated at the melting temperature of the pure component.

The pair interaction energy between two nonidentical molecules is given by

$$\lambda_{ij} = \lambda_{ji} = \lambda_{ii} \quad (9)$$

where i is the compound with the shorter alkyl chain of the pair ij .

Alternatively we also tested a more simple approach to the description of the solidus line measured assuming that the solid phase forming is essentially a pure fatty acid ester and that the liquid phase is ideal. On the basis of these assumptions, the relation between the composition of the mixture, x_i , and the melting/cloud point, T , is given by the classical solid liquid equilibrium equation.

$$x_i^L = \exp \left[-\left(\frac{\Delta_{\text{fus}}H_i}{R} \left(\frac{1}{T} - \frac{T}{T_{\text{fus},i}} \right) \right) \right] \quad (10)$$

The solid–liquid equilibrium models adopted here are predictive models that use, in the calculation of the phase behavior, only pure component properties. Correlations for the thermophysical properties of fatty acid esters were proposed in a previous work.³ The most adequate estimates for the critical temperature (T_c) and pressure (P_c) of saturated ethyl esters are obtained by using the Nikitin et al.³³ correlation. For the acentric factor (ω), the Hang and Peng³⁴ model was found to be the most adequate. The values used in this work, based on these correlations, are reported in Table 1.

The melting temperatures (T_{fus}) of the saturated and unsaturated ethyl esters were obtained directly from the experimental thermograms.

The correlations used for the estimation of the fusion ($\Delta_{\text{fus}}H$) and vaporization enthalpies ($\Delta_{\text{vap}}H$) of saturated ethyl esters were, respectively³

$$\Delta_{\text{fus}}H = 3.92C_n + 16.80 \quad (11)$$

$$\Delta_{\text{vap}}H = 4.9C_n + 9.0 \quad (12)$$

where the enthalpies are expressed in kJ mol^{-1} . For the unsaturated ethyl esters it was assumed that the differences between the fusion ($\Delta_{\text{fus}}H$) and vaporization enthalpies ($\Delta_{\text{vap}}H$) of the saturated and unsaturated methyl esters would be the same as those observed for the ethyl esters.³

Results and Discussion

As discussed in a previous work,³ there is a dramatic lack of experimental data of cloud points of well-characterized

(28) Coutinho, J. A. P.; Knudsen, K.; Andersen, S. I.; Stenby, E. H. *Chem. Eng. Sci.* **1996**, *51*, 3273–3282.

(29) Coutinho, J. A. P.; Stenby, E. H. *Ind. Eng. Chem. Res.* **1996**, *35*, 918–925.

(30) Coutinho, J. A. P.; Ruffier-Meray, V. *Ind. Eng. Chem. Res.* **1997**, *36*, 4977–4983.

(31) Coutinho, J. A. P. *Ind. Eng. Chem. Res.* **1998**, *37*, 4870–4875.

(32) Coutinho, J. A. P. *Fluid Phase Equilib.* **1999**, *160*, 447–457.

(33) Nikitin, E. D.; Pavlov, P. A.; Bogatishcheva, N. S. *Fluid Phase Equilib.* **2005**, *235*, 1–6.

(34) Han, B.; Peng, D. *Can. J. Chem. Eng.* **1993**, *71*, 332–333.

Table 2. Melting Points for the Binary Systems of Saturated Ethyl Esters with Ethyl Stearate

ethyl caprilate + ethyl estearate		ethyl caprate + ethyl estearate		ethyl laurate + ethyl estearate		ethyl miristate + ethyl estearate		ethyl palmitate + ethyl estearate	
$x_{C10:0}$	T (K)	$x_{C12:0}$	T (K)	$x_{C14:0}$	T (K)	$x_{C16:0}$	T (K)	$x_{C18:0}$	T (K)
0.0000	307.93	0.0000	307.93	0.0000	307.93	0.0000	307.93	0.0000	307.93
0.1152	306.59	0.0951	306.35	0.2037	304.77	0.1154	305.88	0.0980	305.96
0.2026	304.93	0.2201	304.64	0.3121	303.16	0.2386	303.99	0.2032	303.64
0.2978	303.23	0.2980	304.01	0.3999	302.10	0.3054	302.86	0.2763	302.81
0.4301	301.33	0.3975	301.39	0.4963	300.55	0.4045	300.95	0.3774	300.56
0.4804	299.58	0.4842	299.91	0.6089	298.04	0.5069	298.25	0.5365	298.79
0.6000	296.87	0.6190	295.43	0.6815	296.39	0.6355	294.97	0.6109	297.78
0.6849	293.37	0.7137	292.74	0.7567	293.35	0.7054	291.74	0.7063	296.82
0.7739	290.11	0.8208	286.65	0.8807	283.64	0.7822	286.40	0.8005	295.67
0.8824	283.88	0.8960	281.82	1.0000	272.51	0.8830	283.37	0.8820	294.97
1.0000	228.19	1.0000	254.51			1.0000	285.74	1.0000	297.74

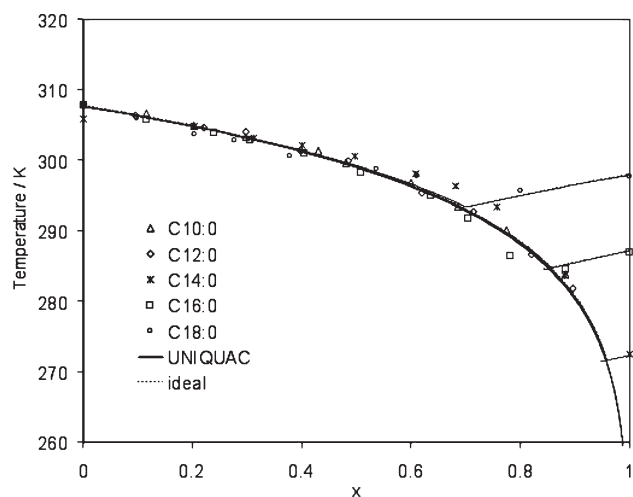
biodiesel mixtures in the open literature what makes the development and test of cloud point models very difficult. To overcome this limitation, melting points for five systems of saturated ethyl esters and two systems of unsaturated ethyl esters with ethyl stearate were measured by DSC, in a total of seven systems that cover all the binary mixtures of the most common ethyl esters with ethyl stearate, one of the heaviest fatty acid esters that may be found in biodiesel produced from virgin vegetable oils. The experimental data is reported in Tables 2 and 3.

The melting points of the mixtures studied seem to indicate that these systems present simple phase diagrams with or without eutectic points. The eutectic point seems to be present whenever the difference between the melting points of the two esters is inferior to 45 K. In the other cases no eutectic point was observed. A careful analysis of the phase diagrams of the heavier esters seems to indicate the presence of peritectic points in these systems. The complexity of the thermograms suggests that, as for the binary mixtures of fatty acids studied previously,^{35–37} the phase diagrams below the solidus line could be rather complex. This subject is under investigation and will be subject of a future work.

Unlike for conventional fuels, for which the complexity of their composition does not allow a simple mixture to be taken as representative of these fluids behavior, a B100 biodiesel is a much simpler fluid that in the limit may have no more than two or three major different esters. The binaries here presented can thus be taken as representative of a B100 biodiesel. The phase diagrams presented in Figures 1 and 2 show that the melting/cloud points are completely dominated by the ethyl stearate and that the unsaturated and light esters, in what concerns the cloud points, act solely as solvents in a biodiesel. Moreover, it should be noticed that the melting/cloud points of the systems studied overlap in almost the entire concentration range, meaning that there is no different between the solvents on the cloud points when the concentrations are expressed in molar fractions. It is also quite interesting to notice how much the presence of the heavy ester impacts on the melting/cloud point of the mixture. It only departs more than 5 K from the melting point of the ethyl stearate when its

Table 3. Melting Points for the Binary Systems of Unsaturated Ethyl Esters with Ethyl Stearate

ethyl oleate + ethyl estearate		ethyl linoleate + ethyl estearate	
$x_{C20:1}$	T (K)	$x_{C20:2}$	T (K)
0.0000	307.93	0.0000	307.93
0.1053	306.29	0.1026	306.63
0.2119	304.83	0.1841	304.97
0.3121	302.80	0.3054	303.60
0.4204	301.41	0.4062	301.30
0.4755	300.54	0.5063	299.16
0.5851	298.28	0.5748	298.32
0.6875	295.27	0.6789	295.44
0.7865	291.40	0.7797	291.61
0.9026	283.06	0.8998	281.20
1.0000	254.61	1.0000	220.68

**Figure 1.** Experimental and predicted melting points for the binary mixtures of ethyl caprilate, ethyl caprate, ethyl laurate, ethyl miristate, or ethyl palmitate with ethyl stearate.

concentration drops below 40%. This suggests that dilution with a solvent is not a very efficient procedure to control the cloud point of a biodiesel. Moreover, if the solvents have a similar effect when the solubility is expressed in mol fractions, then the solvent capability expressed in mass or volume fractions will be inversely proportional to the molecular weight of the solvent, thus solvents with low molecular weight should be preferred to decrease the cloud points of biodiesels.

The data here reported was used to test the Predictive UNIQUAC model previously proposed for the prediction of cloud points of diesels and crude oils.^{8–22} The model was used in a previous work for the description of fatty acid methyl

(35) Costa, M. C.; Sardo, M.; Rolemberg, Marlus P.; Krahenbuhl, M. A.; Meirelles, A. J. A.; Ribeiro-Claro, P.; Coutinho, J. A. P. *Chem. Phys. Lipids* **2009**, *157*, 40–50.

(36) Costa, M. C.; Sardo, M.; Rolemberg, Marlus P.; Krahenbuhl, M. A.; Meirelles, A. J. A.; Ribeiro-Claro, P.; Coutinho, J. A. P. *Chem. Phys. Lipids* **2009**, *160*, 85–97.

(37) Costa, M. C.; Rolemberg, Marlus P.; Meirelles, A. J. A.; Coutinho, J. A. P.; Krahenbuhl, M. A. *Thermochim. Acta* **2009** (DOI information: 10.1016/j.tca.2009.06.018).

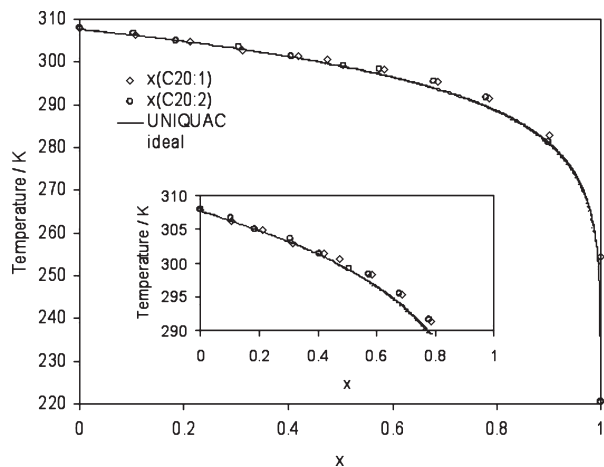


Figure 2. Experimental and predicted melting points for the binary mixtures of ethyl oleate or ethyl linoleate with ethyl stearate.

esters³ and will now be extended to fatty acid ethyl esters. Since this model is part of some commercial or in-house simulators it is important to evaluate its capability concerning the behavior of biofuels. As shown below, an alternative and simpler approach to the prediction of the melting points here reported could provide a good description of the experimental data reported and could probably also describe the behavior of a B100. However, since biodiesel is commercialized essentially as Bx mixtures with conventional diesel, the ideal model, unlike the Predictive UNIQUAC model here used, is not applicable to these complex mixtures of hydrocarbons and fatty acid esters.

The full lines presented in Figures 1 and 2 are the predictions of the melting points of these mixtures obtained using the Predictive UNIQUAC model. As can be observed, the model provides an excellent description of the experimental data measured with an average deviation inferior to 0.5 K. There is no degradation of the quality of the predictions between the mixtures of saturated esters and the mixtures with oleate or linoleate even at very low temperatures. These results are in agreement with what had been previously obtained for fatty acid methyl ester mixtures³ and show the ability of this model to describe the low-temperature behavior of biodiesel.

An alternative approach to the description of these data was also attempted here assuming an ideal mixture in the liquid phase and a pure solid phase. The relations between the melting temperature of the mixture, T , and its composition, x , is given by eq 10. This approach is also predictive as no fitting parameters are required to describe the experimental data. Only melting temperatures and enthalpies of the pure compounds are required to use this model. The results obtained, reported on Figures 1 and 2 as dashed lines, are surprisingly good and essentially identical to those obtained using the more complex approach based on the Predictive UNIQUAC model. Although this approach can hardly apply to a Bx mixture, it may still hold for more complex mixtures of fatty acid esters and thus allow the prediction of cloud points of biodiesel from the knowledge of their composition. A detailed analysis of the potential of this approach to real biodiesel will be object of a future work.

Conclusion

Melting/cloud points for seven binary mixtures of saturated and unsaturated fatty acid ethyl esters with ethyl stearate were measured by DSC and are here reported. These data allow a better understanding of the impact of the heavier fatty acid esters content on the low temperature behavior of biodiesel. It is expected that these data will also contribute to the development and test of models to describe the low temperature behavior of biodiesel.

The Predictive UNIQUAC model, developed for the prediction of cloud points of diesels and previously applied to fatty acid methyl esters, is shown to produce an excellent prediction of the experimental data measured in this work. A simple ideal solution model is shown to be able to describe the melting points with identical accuracy to the Predictive UNIQUAC model and may prove to be able to describe real biodiesel.

Acknowledgment. The authors are grateful to CNPq (306250/2007-1 and 303649/2004-6), FAPESP (05/53095-2, 08/09502-0, 08/56258-8), CAPES-GRICES (0148/06-7), and FAEPEX/UNICAMP for financial support. This work was also supported by FEDER and Fundação para a Ciência e Tecnologia through project POCI/CTM/60288/2004.